Edge transport properties of the fractional quantum Hall states and weak-impurity scattering of a one-dimensional charge-density wave

Xiao-Gang Wen*
School of Natural Science, Institute for Advanced Study, Princeton, New Jersey 08540
(Received 11 March 1991)

Static and dynamical transport properties of the fractional quantum Hall (FQH) states are studied based on the theory of the edge excitations. Because the electrons on the edge of the FQH states are strongly correlated, the *I-V* curve is, in general, nonlinear and contains singular structures. A narrow-band noise is found in the dc transport of the FQH states, which can be used to directly measure the fractional charge of the quasiparticles. The long-range Coulomb interaction is also discussed, which is found to have a profound effect on the transport properties of the integer quantum Hall and FQH states. In particular, the long-range interaction will cause a breakdown of the quantized conductance in narrow quantum Hall samples. As a closely related problem, we also study the transport properties of a one-dimensional charge-density-wave state in the presence of a single weak impurity. An exact mapping between two-dimensional quantum Hall systems and one-dimensional electron models is found.

It is well known that the quantum Hall (QH) states do not support any gapless bulk excitations. All the low-lying excitations appear only near the edges of samples.[1-3] At low temperatures the density of the bulk excitations is exponentially small. Thus the transport properties of the QH states are governed by the edge excitations at low temperatures.[4,5] Due to the chiral structure of the edge excitations, there is no backscattering and a static current on a single edge cannot cause a voltage drop along the edge. (This is a result of the charge conservation.) The voltage drop can appear only if (A) the edge excitations interact with the bulk excitations or (B) edge excitations tunnel from one edge to another. The effect (A) can be ignored at low temperatures. In this paper we will concentrate on the effect (B), i.e., the transport arising from the tunneling between the edge states.

In the past two years, a lot of progress was made in theoretical understanding of the edge excitations in the fractional quantum Hall (FQH) effects. The chiral dynamical properties of the edge excitations were studied in Refs. 2, 6 and 8. The electron propagator along the edge was calculated in Ref. 9 and confirmed numerically in Ref. 8. The relation between the edge excitations and the microscopic electron wave function was discussed in Refs. 10, 7, 9, and 8. The structures of the edge excitations in the hierarchical FQH states and non-Abelian FQH states were studied in Refs. 3, 11, and 12. The edge states for spin-$\frac{1}{2}$ electrons were obtained in Refs. 2 and 13. Those theoretical advances make it possible to obtain quantitative tunneling properties for various FQH states. Recent developments on the fabrication of the devices at 1000-Å scale also make it possible to experimentally study in detail the tunneling between edge states. Thus it is interesting to calculate some curves quantitatively for realistic situations. Hopefully those theoretical predictions can be tested in the near future.

We also study a closely related problem: the scattering of a drifting one-dimensional (1D) charge-density wave (CDW) by a single weak impurity. Impurity pinning of a 1D CDW has been studied in detail in Refs. 14 and 15. In this paper we will concentrate on the effects of quantum fluctuations in a situation where the voltage acting on the CDW is much larger than the pinning threshold. Some recent experiments on 1D electron systems can be found in Ref. 16.

The paper is arranged as follows. In Sec. I we study the transport properties of the simple Laughlin states. In this section we assume that the excitations on different edges do not interact with each other. In Sec. II we study the effects of interedge interactions (including the effects of the long-range Coulomb interaction) on the transport properties. A relation between the transport in FQH systems and the transport in one-dimensional CDW systems is pointed out. In Sec. III an exact mapping between two-dimensionals QH systems and one-dimensional models with short-range interactions is discussed. Section IV contains some discussions and conclusions.

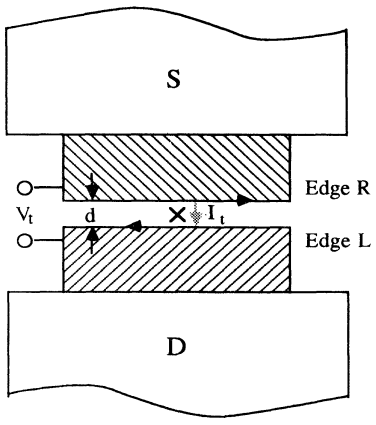

FIG. 1. Tunneling junction of two QH system. × marks the position of the impurity.

I. TRANSPORT IN THE FQH STATES IN THE ABSENCE OF THE COULOMB INTERACTION

In this section we will assume electrons in the QH states have only short-range interactions. Such a situation can be realized in experiments by putting a metallic film near the two-dimensional electron gas to screen away the Coulomb interaction.

First let us study the tunneling between the edges of two *different* FQH samples (see Fig. 1). Since the electrons on edges L and R have different k_x momenta: $k_x(L)-k_x(R)\equiv k_0=d/l^2$ ($l=\sqrt{\hbar c/eB}$ is the magnetic length), the tunneling between the two edges can happen only with the assistance of impurities, phonons, or other interactions which can absorb the extra momentum. In this paper we will only consider the impurity assisted tunneling. We will also limit ourself to the tunneling at low voltages and low temperatures so that the retardation of the tunneling can be ignored. (We will not consider the resonant tunneling.[5]) Because the electron interaction is short ranged, we will assume in this section that the excitations on different edges do not interact with each other.

Let us consider a simple case where the tunneling is assisted by a single impurity at $x=0$. The tunneling operator can now be written as $\Gamma A=\Gamma c_L c_R^\dagger|_{x=0}$, where $c_{R,L}$ are the electron operators on edges R and L. The tunneling current between the two edges I_t is given by the formula[17]

$$I_t(t)=e\Gamma^2\int_{-\infty}^{+\infty}dt'\Theta(t-t')\left[\exp\left[i\int_t^{t'}eV_t(\tilde{t})d\tilde{t}\right]\langle[A(t),A^\dagger(t')]\rangle-\exp\left[-i\int_t^{t'}eV_t(\tilde{t})d\tilde{t}\right]\langle[A^\dagger(t),A(t')]\rangle\right], \quad (1)$$

where V_t is the voltage difference between the two edges. Introducing $f(\omega,t)$ through

$$\exp\left[i\int_t^{t'}eV_t(\tilde{t})d\tilde{t}\right]=\int d\omega\, f(\omega,t)e^{i(t-\tilde{t})\omega} \quad (2)$$

we find that (1) can be rewritten as

$$I_t(t)=-2e\Gamma^2\int d\omega\,\mathrm{Im}[f(\omega,t)X_{\mathrm{ret}}(-\omega)], \quad (3)$$

where X_{ret} is defined by

$$X_{\mathrm{ret}}(t)=-i\theta(t)\langle[A(t),A^\dagger(0)]\rangle. \quad (4)$$

For a dc voltage, (3) is simplified to

$$I_t=-2e\Gamma^2\,\mathrm{Im}[X_{\mathrm{ret}}(-eV_t)]. \quad (5)$$

Notice that (1) is just the leading term in the expansion of the tunneling amplitude Γ. In this paper we will limit ourself to weak tunneling situations and keep only the leading term.

Formula (1) reduces the tunneling problem to a calculation of the correlation function of the tunneling operator A. In the rest of the paper we will use the theory of the edge states to calculate such a correlation function in various situations. Then we will use (1) to obtain various tunneling I-V curves.

The electron propagator along the edges of the FQH states has been evaluated in Refs. 9 and 11. For the simple Laughlin state of filling fraction $\nu=1/q$, the propagator is given by

$$\langle c_{R,L}^\dagger(x,t)c_{R,L}(0)\rangle\propto(x\mp vt)^{-g}e^{\pm i\nu^{-1}k_Fx} \quad (6)$$

at zero temperature. Here $g=1/\nu=q$ is an odd integer, v is the velocity of the edge excitations, and $k_F=2\pi nd=\nu k_0$. (n is the two-dimensional electron density.) Because the excitations on the two edges do not interact with each other, the propagator of the tunneling operator A can be calculated from (6):

$$\begin{aligned}G_+(x,t)&=\langle A(x,t)A^\dagger(0)\rangle\\&=a^{g-2}[x^2-v^2(t-i\delta)^2]^{-g}e^{2i\nu^{-1}k_Fx},\\G_-(x,t)&=\langle A^\dagger(0)A(x,t)\rangle\\&=a^{g-2}[x^2-v^2(t+i\delta)^2]^{-g}e^{2i\nu^{-1}k_Fx},\end{aligned} \quad (7)$$

where a is the cutoff length scale whose value will be discussed later. The retarded Green function X_{ret} is given by

$$\begin{aligned}X_{\mathrm{ret}}(\omega)&=\int-i\Theta(t)[G_+(x,t)-G_-(x,t)]e^{i\omega t}dt\\&=a^{2g-2}v^{-2g}|\omega|^{2g-1}\\&\quad\times\frac{\pi}{\Gamma(2g)}[\tan(\pi g)+i\,\mathrm{sgn}(\omega)].\end{aligned} \quad (8)$$

For the Laughlin state, g is an odd integer q and (8) can be further simplified to

$$X_{\mathrm{ret}}(\omega)=-i\frac{\pi}{(2q-1)!}a^{2q-2}v^{-2q}\omega^{2q-1}. \quad (9)$$

Equations (9) and (5) imply that the dc tunneling current is given by $I_t\propto V_t^{2q-1}$, which is *nonlinear*. The nonlinear I_t-V_t curve is a consequence of the strong correlation in the FQH states. We notice that the I_t-V_t curve for the $\nu=1$ integer quantum Hall (IQH) state ($q=1$) is linear. This is because the edge excitations in the IQH states are described by the Fermi-liquid theory.

Now let us consider a situation where V_t has an ac component:

$$V_t(t)=V_0+V_1\sin(\Omega t). \quad (10)$$

In this case the time average $f(\omega,t)$,

$$\bar{f}(\omega)=\frac{\Omega}{2\pi}\int_0^{2\pi/\Omega}dt\,f(\omega,t),$$

has a form

$$\bar{f}(\omega)=\sum_{n=-\infty}^{\infty} a_n \delta(eV_0+n\Omega-\omega) . \tag{11}$$

It is easy to see that $a_n=a_{-n}$ are real and a_n only depend on the ratio $\xi=eV_1/\Omega$. In fact we have

$$a_n(\xi)=\frac{1}{4\pi^2}\int_0^{2\pi}dt\int_0^{2\pi}dt' e^{in(t'-t)}e^{i\xi(\cos t'-\cos t)} . \tag{12}$$

The dc component of the tunneling current I_t is found to be

$$I_t^{(\mathrm{dc})}\equiv\frac{\Omega}{2\pi}\int_0^{2\pi/\Omega}dt\, I_t(t) \propto \sum_{n=-\infty}^{\infty} a_n(\xi)(eV_0+n\Omega)^{2g-1} . \tag{13}$$

The $I_t^{(\mathrm{dc})}$-V_t curve for a few values of eV_1/Ω is plotted in Fig. 2 where we have chosen $q=3$ (the $\nu=\frac{1}{3}$ Laughlin state). We see that in the presence of an ac component, the tunneling junction develops a nonzero conductance at $V_t=0$.

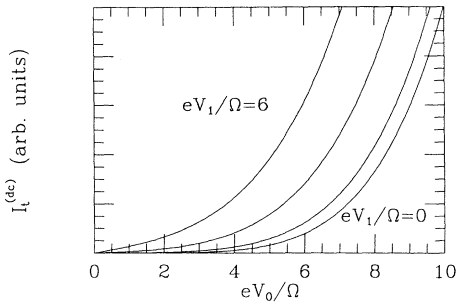

FIG. 2. The $I_t^{(\mathrm{dc})}$-V_0 curve for the $\nu=\frac{1}{3}$ Laughlin state in Fig. 1. The voltage V_t has an ac component of amplitudes $eV_1/\Omega=0,2,4,6$.

The finite-temperature propagators can be obtained from the zero-temperature ones through a conformal transformation.[18] We find that (7) becomes

$$G_+(x,t)=a^{g-2}(\pi T)^{2g}|\sinh[\pi T(x-vt)]\sinh[\pi T(x+vt)]|^{-g}e^{i\pi g\,\mathrm{sgn}(t)\Theta(v^2-x^2)} ,$$
$$G_-(x,t)=a^{g-2}(\pi T)^{2g}|\sinh[\pi T(x-vt)]\sinh[\pi T(x+vt)]|^{-g}e^{-i\pi g\,\mathrm{sgn}(t)\Theta(v^2t^2-x^2)} \tag{14}$$

at finite temperatures. Equation (14) implies

$$X_{\mathrm{ret}}(\omega)=a^{2g-2}v^{-2g}(2\pi T)^{2g-1} \times B(g-i\omega/2\pi T, g+i\omega/2\pi T) \times\frac{\sin[\pi(g+i\omega/2\pi T)]}{\cos(\pi g)} , \tag{15}$$

where B is the beta function. For dc voltage, the I_t-V_t curves at finite temperatures are plotted in Fig. 3 (again we have chosen $q=3$). We see that the differential conductance $(dI_t/dV_t)|V_t=0$ is nonzero at finite temperatures. From (15) we can further show that

$$(dI_t/dV_t)|_{V_t=0}\propto T^{2g-2} . \tag{16}$$

Now let us consider a more interesting device with a geometry as presented in Fig. 4. The low-temperature transport of such a Hall bar is still governed by the tunneling between the two edges. Again we will assume the tunneling is induced by an impurity in the QH sample.

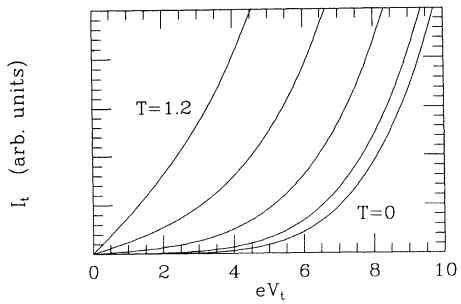

FIG. 3. The dc tunneling I_t-V_t curve for the $\nu=\frac{1}{3}$ Laughlin state in Fig. 1 at finite temperatures $T=0,0.3,0.6,0.9,1.2$. We have chosen $k_B=1$. eV_t and T are measured with the same energy unit.

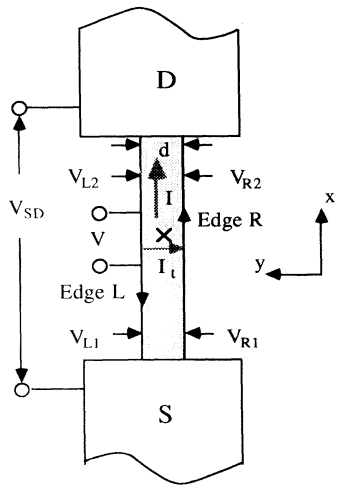

FIG. 4. A Hall bar with an impurity at ×. The electrons in the shaded region form a QH state.

For such a system the tunneling can be accomplished by moving one electron from one edge to the other; it can also be accomplished by moving one quasiparticle between the edges.[19] We know the quasiparticles in the FQH state correspond to vortices of unit flux. The quasiparticles tunneling across the FQH sample in some sense resembles the vortex tunneling across a superconducting stripe. The contribution from the electron tunneling is discussed above. In the following we will concentrate on the quasiparticle tunneling. Again we will only consider a simple Laughlin state as an example.

Some aspects of the quasiparticle tunneling operator have been discussed in Ref. 9. There the Hilbert space of the edge excitations on the two edges of a cylindrical FQH sample was constructed. The Hilbert space contains states which are related by transferring a fractional charge e/q between the two edges (assuming the FQH state has a filling fraction $\nu=1/q$). The transition between those states are realized by the quasiparticle tunneling operators. The quasiparticle tunneling operators can easily be written down by generalizing the discussions in Ref. 9. In the following we will briefly summarize these results.

First let us derive an explicit expression of the quasiparticle tunneling operator. The quasiparticle operator on the edge, $\psi_{R,L}$, creates a localized charge and should satisfy

$$[\rho_{R,L}(x),\psi_{R,L}(x')]=e^{*}\delta(x-x')\psi_{R,L}(x') , \tag{17}$$

where $e^{*}=\nu e$ is the charge of the quasiparticle and $\rho_{R,L}$ are the one-dimensional charge-density operators on the edges R and L. Since $\rho_{R,L}$ satisfy the Kac-Moody algebra,[2,6,8]

$$\begin{aligned}&[\rho_{L,R;k},\rho_{L,R;k'}]=\mp\frac{e^2\nu}{2\pi}k\delta_{k+k'} ,\\ &[\rho_{L,k},\rho_{R,k'}]=0 ,\\ &k,k'=\text{integer}\times\frac{2\pi}{L} ,\end{aligned} \tag{18}$$

one can show that the quasiparticle operators which satisfy (17) are given by[9]

$$\psi_{L,R}\propto e^{\pm i(e^{*}/e\sqrt{\nu})\phi_{L,R}}e^{\pm ik_F x} , \tag{19}$$

where $\phi_{L,R}$ is given by $\rho_{L,R}=e(\sqrt{\nu}/2\pi)\partial_x\phi_{L,R}$. We immediately see that the quasiparticle tunneling operator $A=\psi_R^{\dagger}\psi_L$ is given by

$$A\propto e^{i(e^{*}/e\sqrt{\nu})(\phi_L+\phi_R)}e^{2ik_F x} . \tag{20}$$

We would like to remark that the quasiparticle creation operator $\psi_{R,L}$, creating a fractional charge, is not physical, in the sense that it creates a state outside the physical Hilbert space. However, the quasiparticle tunneling operator A in (20), being a neutral operator, is physical. One can show that[9] it creates a state inside the Hilbert space constructed in Ref. 9. We would like to emphasize that the quasiparticle tunneling operator is physical only when the two edges are connected by the same FQH fluid. If two edges belong to two different FQH fluids, then the quasiparticle tunneling operator will not be physical. In this case only electron tunneling is allowed, which is the situation in Fig. 1.

The low-energy dynamics of the edge excitations is governed by a Hamiltonian which satisfies

$$[H,\rho_{L,R;k}]=\mp vk\rho_{L,R;k} . \tag{21}$$

Such a Hamiltonian has a form

$$H=\frac{2\pi v}{e^2\nu}\sum_{k>0}(\rho_{L,k}\rho_{L,-k}+\rho_{R,k}\rho_{R,-k}) . \tag{22}$$

Using (18) and (21) one can show that the correlation functions of the quasiparticle tunneling operators A are still given by (7) but with a new exponent $g=(e^{*}/e\sqrt{\nu})^2=\nu$. (The momentum factor $e^{i2\nu^{-1}k_F x}$ now becomes $e^{2ik_F x}$.) The tunneling formula (1) also applies to the quasiparticle tunneling after replacing e by e^{*}. Therefore our previous results for the electron tunneling remain valid for the quasiparticle tunneling once e and g are replaced by e^{*} and ν.

Since g is less than $\frac{1}{2}$, the qausiparticle tunneling has very different behaviors than that of the electron tunneling. For example, the zero-temperature dc I_t-V_t curve is given by

$$I_t\propto|V_t|^{2g-1}\text{sgn}(V_t)=|V_t|^{-(q-2)/q}\text{sgn}(V_t) \tag{23}$$

which *diverges* as $V_t\to 0$. Such a diverging tunneling curve resembles the tunneling curve between one-dimensional superconductors (with algebraic decay order parameters). The tunneling curve can be directly measured in experiments by measuring $I=\sigma_{xy}V_t$ and $V=I_t/\sigma_{xy}$ in Fig. 4. Here $\sigma_{xy}=\nu e^2/h$ is the Hall conductance of the FQH state. We would like to remark that our discussions are based on the weak tunneling theory. Our results are valid only when the tunneling current is small: $I_t\ll I$, or equivalently,

$$I_t/V_t\ll\sigma_{xy} . \tag{24}$$

Equation (23) violates (24) at small V_t. In this case (23) is no longer valid and the divergence is expected to be rounded off.

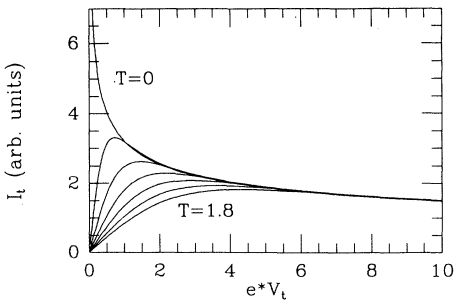

FIG. 5. The dc I_t-V_t tunneling curve for the $\nu=\frac{1}{3}$ Laughlin state in Fig. 4 at finite temperatures $T=0,0.3,0.6,\ldots,1.8$. $e^{*}=\nu e$ is the quasiparticle charge. We have chosen $k_B=1$. $e^{*}V_t$ and T are measured with the same energy unit.

Finite temperatures also remove the divergence. The I_t-V_t curves at finite temperatures are given by (15) and are plotted in Fig. 5. (Again we have chosen $\nu=\frac{1}{3}$.) We see that I_t peaks at a voltage

$$V_{t,\max}=2.38T/e^* . \tag{25}$$

Thus the finite temperature I_t-V_t curve can provide information about the quasiparticle charge e^* once the zero-temperature behavior (23) is confirmed.

It is instructive to calculate the total current I passing through the Hall bar as a function of the voltage difference between the source and the drain: $V_{SD}=V_S-V_D$. We notice that the voltage along an edge has a drop (or rise) when we pass through the tunneling point. We may evaluate V_t using the average of the voltages on the two sides of the tunneling point:

$$V_t=\tfrac{1}{2}(V_{L1}+V_{L2})-\tfrac{1}{2}(V_{R1}+V_{R2})=I/\sigma_{xy} . \tag{26}$$

The voltage V_{SD} now can be calculated as

$$V_{SD}(I)=V_{R1}-V_{L2}=\frac{I_t(V_t)|_{V_t=I/\sigma_{xy}}+I}{\sigma_{xy}} . \tag{27}$$

A typical I-V_{SD} curve and (dI/dV_{SD})-V_{SD} curve are plotted in Fig. 6. The curves show a turning-on structure near a certain threshold V_{SD0}. Notice that at zero temperature the function $V_{SD}(I)$ has a minimum and it turns out that V_{SD0} is the minimum of $V_{SD}(I)$:

$$V_{SD0}=\frac{2}{ea}(1-2g)^{-(1-2g)/(2-2g)}(1-g) \times g^{g/(1+2g)}\left[\frac{\Gamma v^{-g}}{\sqrt{g\Gamma(2g)}}\right]^{-1/(1-g)} . \tag{28}$$

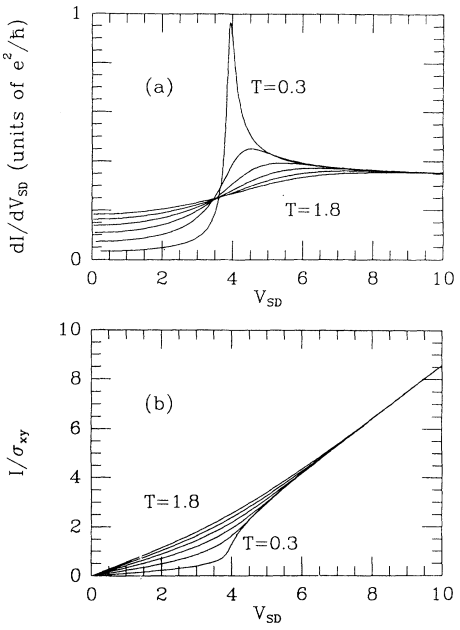

FIG. 6. The (dI/dV_{SD})-V_{SD} curve (a) and the I-V_{SD} curve (b) for the $\nu=\frac{1}{3}$ Laughlin state in Fig. 4 at finite temperatures $T=0.3,0.6,\ldots,1.8$. The unit of the voltage is chosen such that V_{SD0} in (28) is equal to 4. The temperature is measured in units of $e^*V_{SD0}/4$.

The unit of the voltage in Fig. 6 is chosen such that V_{SD0} is equal to 4.

We would like to remark that when $V_{SD}\lesssim V_{SD0}$ the tunneling current is large and our approaches do not apply. The detail features near V_{SD0} in Fig. 6 are not reli-

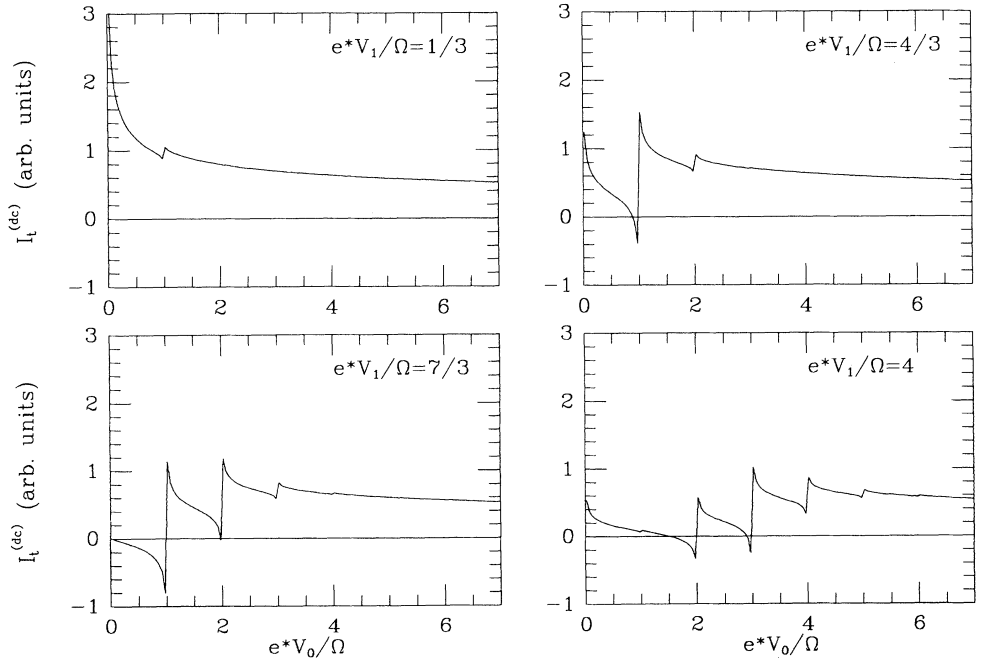

FIG. 7. The $I_t^{(dc)}$-V_0 curve for the $\nu=\frac{1}{3}$ Laughlin state in Fig. 4 with different ac components in V_t. We have chosen the temperature T to be zero and $\hbar=1$.

able. Our results are valid only for $V_{SD} \gg V_{SD0}$. However, our calculations do suggest that as we decrease V_{SD}, there is a sudden drop in the current I near the characteristic voltage V_{SD0}. Such a structure resembles the impurity pinning of one-dimensional incommensurate CDW. A more detailed discussion will be given later.

Now let us consider the situation where V_t has an ac component. The dc component of the tunneling current, $I_t^{(\mathrm{dc})}$, is given by

$$I_t^{(\mathrm{dc})} \propto \sum_{n=-\infty}^{\infty} a_n(\xi)\mathrm{Im}X_{\mathrm{ret}}(e^*V_0+n\Omega) ,$$
$$\xi = e^*V_1/\Omega \tag{29}$$

which is plotted in Fig. 7 for a few values of e^*V_1/Ω. In Fig. 7 we have chosen $\nu=\frac{1}{3}$ and $T=0$. We see that there are many resonance structures at integer values of e^*V_0/Ω. Those structures provide a *direct* measurement of the quasiparticle charge. The resonance structures in the tunneling between the two edge states resemble the Josephson effects between superconductors. Later we will see that the resonance structures in Fig. 7 reflect the existence of narrow-band noise in dc transport, which is very similar to the narrow-band noise in CDW transport. Probably a more direct way to measure the quasiparticle charge is to measure the frequency of the narrow-band noise which is given by $\Omega_{ns}=e^*V_t/\hbar$.

To see whether it is possible to observe the resonance structures in experiments, let us make some numerical estimates. Assume $\Omega=2$ GHz. To observe the resonances, V_0 and V_1 should be of order $\Omega\hbar/e^* \sim 30$ μV. The current passing through the Hall bar, I, is of order 0.4 nA. The tunneling current I_t can be measured by measuring V in Fig. 4. The validity of our results requires $V \ll V_0$. Thus the sensitivity of the measurement of V should be much better than 30 μV, which is achievable. Thus it may be possible to observe the resonances in experiments and give a direct measurement of the quasiparticle charge.

II. TRANSPORT IN THE PRESENCE OF THE COULOMB INTERACTION

The tunneling effects discussed in the preceding section are easy to observe when the two edges are close to each other. In this case the interactions between excitations on the different edges cannot be ignored, in particular when the long-range Coulomb interaction is present. In this section we will discuss the effects of these interactions on the edge transport properties of the FQH states.

Let us concentrate on the system in Fig. 4. The Hilbert space of the low-lying edge excitations is still generated by the Kac-Moody algebra (18), but the Hamiltonian is no longer given by (22). In presence of the interaction the Hamiltonian becomes

$$H=\frac{2\pi v}{e^2\nu}\sum_{k>0}(\rho_{L,k}\rho_{L,-k}+\rho_{R,k}\rho_{R,-k})+\sum_{k>0}V_1(k)(\rho_{L,k}\rho_{L,-k}+\rho_{R,k}\rho_{R,-k})$$
$$+\sum_{k>0}V_2(k)(\rho_{R,k}\rho_{L,-k}+\rho_{L,k}\rho_{R,-k})+\left[\frac{\pi v}{e^2\nu}+\tfrac{1}{2}V_1(0)\right](\rho_{L,0}^2+\rho_{R,0}^2)+V_2(0)\rho_{R,0}\rho_{L,0} . \tag{30}$$

Here V_1 represents an intraedge interaction and V_2 an interedge interaction. In (30) we have included the zero momentum component of the density. Notice that, at low energies, the intraedge interaction $V_1(k)$ can only modify the edge velocity if $V_1(k)$ is finite as $k\to 0$. In this case the V_1 term can be absorbed in the first term in (30). The intraedge interaction can give rise to new features only when $V_1(k)\to\infty$ as $k\to 0$. In contrast, as we will see, the interedge interaction will have drastic effects even when $V_2(k)$ is finite.

Even in the presence of the interactions, dynamics of the edge states described by (18) and (30) is still exactly soluble. Introducing

$$\tilde{\rho}_{L,k}=\cosh\theta_k\rho_{L,k}+\sinh\theta_k\rho_{R,k} ,$$
$$\tilde{\rho}_{R,k}=\cosh\theta_k\rho_{R,k}+\sinh\theta_k\rho_{L,k} \tag{31}$$

we find $\tilde{\rho}_{L,R}$ still satisfy the Kac-Moody algebra:

$$[\tilde{\rho}_{L,R;k},\tilde{\rho}_{L,R;k'}]=\mp\frac{e^2\nu}{2\pi}k\delta_{k+k'} ,$$
$$[\tilde{\rho}_{L,k},\tilde{\rho}_{R,k'}]=0 . \tag{32}$$

If we further choose θ_k to satisfy

$$\tanh 2\theta_k=\frac{V_2(k)}{2\pi\nu/e^2\nu+V_1(k)} \tag{33}$$

then the Hamiltonian (30) will have the following diagonal form:

$$H=\frac{2\pi}{e^2\nu}\sum_{k>0}\tilde{v}_k(\tilde{\rho}_{L,k}\tilde{\rho}_{L,-k}+\tilde{\rho}_{R,k}\tilde{\rho}_{R,-k})$$
$$+\frac{\pi\tilde{v}_0}{e^2\nu}(\tilde{\rho}_{L,0}^2+\rho_{R,0}^{-2}) , \tag{34}$$

where

$$\tilde{v}_k^2=\left[v+\frac{\nu e^2V_1(k)}{2\pi}\right]^2-\left[\frac{\nu e^2V_2(k)}{2\pi}\right]^2 . \tag{35}$$

Equations (32) and (34) imply that

$$[H,\tilde{\rho}_{L,R;k}]=\mp\tilde{v}_k k\tilde{\rho}_{L,R;k} . \tag{36}$$

Equations (32) and (36) describe a collection of noninteracting oscillators and hence are exactly soluble. The

dispersion relation for the edge excitations is given by $\varepsilon_k = \tilde{v}_k k$.

First let us assume there are no impurities and study the effects of the interactions on the transport properties of the clean Hall bar. In the presence of the interedge interaction, the excitations on edges L and R are mixed. The right (left) moving excitations generated by $\tilde{\rho}_R$ ($\tilde{\rho}_L$) are no longer localized on edge R (L). In this case one needs to define various quantities carefully. The total current and the total charge on the Hall bar are given by

$$\begin{aligned} Q &= \sqrt{L}\,(\rho_{R,0}+\rho_{L,0}) \\ &= \sqrt{L}\,(\cosh\theta_0-\sinh\theta_0)(\tilde{\rho}_{R,0}+\tilde{\rho}_{L,0})\ , \\ I &= \frac{\tilde{v}_0}{\sqrt{L}}(\cosh\theta_0-\sinh\theta_0)(\tilde{\rho}_{R,0}-\tilde{\rho}_{L,0})\ . \end{aligned} \tag{37}$$

Thus the charge density of the right movers is given by $(\cosh\theta_0-\sinh\theta_0)\tilde{\rho}_R/\sqrt{L}$ and left movers by $(\cosh\theta_0-\sinh\theta_0)\tilde{\rho}_L/\sqrt{L}$. The voltage V_t is the voltage difference between the excitations on the edges R and L, which is given by

$$V_t = \frac{1}{\sqrt{L}}\left[\frac{\partial H}{\partial \rho_{R,0}} - \frac{\partial H}{\partial \rho_{L,0}}\right], \tag{38}$$

while voltage V_{SD} is the voltage difference between the right movers and the left movers. V_{SD} is given by

$$V_{SD} = \frac{1}{\sqrt{L}\,(\cosh\theta_0-\sinh\theta_0)}\left[\frac{\partial H}{\partial \tilde{\rho}_{R,0}} - \frac{\partial H}{\partial \tilde{\rho}_{L,0}}\right]. \tag{39}$$

Equations (37)–(39) imply

$$\frac{I}{V_{SD}} = e^{-2\theta_0}\frac{\nu e^2}{h},\quad \frac{V_t}{V_{SD}} = e^{-2\theta_0},\quad \frac{I}{V_t} = \frac{\nu e^2}{h}\ . \tag{40}$$

We see in the presence of the interedge interaction we no longer have $V_t = V_{SD}$ and $I/V_{SD} = \nu e^2/h$. The two probe measurement no longer gives the quantized Hall conductance. However, the ratio I/V_t, not affected by any interaction, is still quantized and universal. When we have a small tunneling current I_t across the edges, the voltage drop V along an edge is given by $V = I_t e^{2\theta_0} h/\nu e^2$ which is different from the noninteracting one, $V = I_t h/\nu e^2$.

To understand the generic effects of the interedge interaction on the tunneling, let us first study a simple case in which $V_1, V_2 = \text{const}$. Now $\theta_k = \theta$ and $\tilde{v}_k = \tilde{v}$ are independent of k. The quasiparticle tunneling operator (20), when expressed in terms of $\tilde{\rho}_{L,R}$, has a form

$$\psi_R^\dagger \psi_L \propto e^{i(e^*/e\sqrt{\nu})(\cosh\theta-\sinh\theta)(\tilde{\phi}_L+\tilde{\phi}_R)} e^{i2k_F x}\ , \tag{41}$$

where $\tilde{\phi}_{L,R}$ is given by $\tilde{\rho}_{L,R} = e(\sqrt{\nu}/2\pi)\partial_x \tilde{\phi}_{L,R}$. Thus the correlation functions between the tunneling operators are still given by (14) (with v replaced by $\tilde{v}$), but now the exponent is given by

$$g = \nu(\cosh\theta-\sinh\theta)^2\ . \tag{42}$$

The transport properties can easily be calculated by repeating the procedures in the preceding section. In particular, (8), (13), (15), (16), and (23) remain valid with the new value of g. When $g < \frac{1}{2}$, I_t diverges as $V_t \to 0$ and the transport properties still have the qualitative features as represented in Figs. 5–7. Since $\theta > 0$ for a repulsive interedge interaction, the repulsive interaction reduces the value of g which in turn enhances the tunneling current I_t at small V_t. Even for the $\nu = 1$ IQH state, the repulsive interaction will make $I_t/V_t \to \infty$ as $V_t \to 0$.

We would like to point out that the tunneling formula (1) is still valid even when the electrons on the two edges interact with each other. In general the total Hamiltonian of the system has a form $H_0 + H_t$, where $H_t = \Gamma(\psi_R^\dagger \psi_L + \text{H.c.})$ is the tunneling term and H_0 may contain interedge interactions. Formula (1) applies as long as H_0 commutes with N_L and N_R, the total electron number operators on the two edges.

For the $\nu = 1$ IQH state, g may be in the range $\frac{1}{2} < g < 1$ for a weak repulsive interaction. (Now the quasiparticle operators $\psi_{L,R}$ are the electron operators $c_{L,R}$.) In this case the tunneling current I_t does not diverge as $V_t \to 0$ [see (23)]. But the differential conductance dI_t/dV_t approaches infinity at zero V_t. Thus in the presence of an ac component the differential conductance will show similar resonance structures as demonstrated in Fig. 7.

We would like to point out that resonance structures in Fig. 7 are generic properties of interacting one-dimensional systems with both right and left movers. The exponent g in general depends on the interactions and can take any real values. (For this to be true both the right movers and the left movers must be present.) As long as g is not equal to an integer, similar resonance structures will appear in certain order of derivative of $I_t(V_t)$. From this point of view it seems too limited to only connect the resonances in Fig. 7 to the Josephson effect. The structures in Fig. 7 are generic many-body effects which may appear in many interacting systems even when the superconducting correlation is suppressed.

We would like to remark that for the $\nu = 1$ IQH state, the low-lying edge excitations in the system in Fig. 4 can be mapped to those in the one-dimensional Fermi liquid. The excitations on edges L and R correspond to the excitations near the two Fermi points. Equation (30) in this case actually describes an interacting spinless fermion system in one dimension. The Fermi momentum is given by $k_F = d/2l^2$. The tunneling operator $c_R^\dagger c_L$ carrying a momentum $2k_F$ is the CDW order parameter. From (7) we see that there is a long-range CDW correlation when g is close to 0. It is precisely in this case that we observe a threshold structure in the longitudinal conductance of the system (Fig. 6). This suggests that the threshold in Fig. 6 should be attributed to the impurity pinning of the CDW state. According to our picture, a drifting CDW is realized by letting $\rho_L \neq \rho_R$. The impurity pinning is realized through the tunneling between left movers and right

movers (or by backscattering). Certainly the genuine (incommensurate) CDW state does not exist in one dimension. Here by "CDW state" we mean that the CDW order parameter has a slow algebraic decay (e.g., $g<\frac{1}{2}$). The tunneling picture of impurity scattering of CDW was first proposed in Ref. 15. However, the CDW state in Ref. 15 was treated within a mean-field picture. In this picture we take into account the effects of quantum fluctuations and strong correlations. As a result of strong correlations and quantum fluctuations, the transport properties of the CDW's have nontrivial power-law structure (see the formula at the end of the paper). A renormalization-group study of impurity pinning of 1D CDW's can be found in Ref. 20.

Our formalism also applies to the Coulomb interaction. In this case

$$V_1(k)=2K_0(|k|a)|_{k\to 0}=\frac{2}{\epsilon}\ln\left[\frac{2}{|k|a}\right],$$
$$V_2(k)=2K_0(|k|d)|_{k\to 0}=\frac{2}{\epsilon}\ln\left[\frac{2}{|k|d}\right], \tag{43}$$

where $K_0(k)=\int_0^\infty (x^2+1)^{-1/2}\cos(kx)dx$ is the Basset function and ϵ is the dielectric constant. Now θ_k and $\tilde{v}_k$ in (33) and (35) depend on k.

The correlation between the quasiparticle tunneling operator

$$A=\exp\left[\frac{e^*}{e\sqrt{\nu}}\phi\right] \quad \text{where } \phi=\phi_R+\phi_L$$

is given by

$$G_+(x,t)=e^{\nu\langle\phi(x,t)\phi(0)\rangle}=G_0^*(x,t),$$
$$X_{\rm ret}(t)=2e^{\nu\,{\rm Re}\langle\phi(0,t)\phi(0)\rangle}\sin[\nu\,{\rm Im}\langle\phi(0,t)\phi(0)\rangle], \tag{44}$$
$$\langle\phi(x,t)\phi(0)\rangle=\int_0^{a^{-1}}\frac{e^{-2\theta_k}}{k}(e^{ik(\tilde{v}_k t-x)}+e^{ik(\tilde{v}_k t+x)}-2)dk.$$

The exact value of the above integration is hard to calculate. In the following we will discuss the asymptotic behavior of the above correlation functions.

First let us consider the long-wavelength limit $k<1/d$. In this case θ_k and $\tilde{v}_k$ have the form

$$e^{-2\theta_k}\approx\left[\frac{\ln(d/a)}{2\ln(2/ka)}\right]^{1/2},$$
$$\tilde{v}_k\approx\nu\frac{\alpha c}{\epsilon\pi}\left[\ln\left[\frac{d}{a}\right]\ln\left[\frac{4}{k^2ad}\right]\right]^{1/2}, \tag{45}$$

where $\alpha=\frac{1}{137}$ is the fine-structure constant and c the speed of light. We also have chosen v in (33) and (35) to be zero. (v can always be absorbed in V_1 by redefining a.) We find $\langle\phi(x,t)\phi(0)\rangle$ has the following asymptotic form for large t:

$$\langle\phi(0,t)\phi(0)\rangle|_{x=0}\approx-\left[\frac{1}{2}\ln\frac{d}{a}\right]^{1/2}\left[4\left[\ln\frac{2v_1t}{a^*}\right]^{1/2}+i\pi\left[\ln\frac{2v_1t}{a^*}\right]^{-1/2}\right]+\text{const}, \tag{46}$$

where $V_1=\nu(\alpha c/\epsilon\pi)[2\ln(d/a)]^{1/2}$. Note a^* may not be equal to a due to the possible next-order corrections. After a calculation, the asymptotic form of the propagator $X_{\rm ret}(\omega)$ for small ω is found to be

$${\rm Im}X_{\rm ret}(\omega)\approx C_1\frac{\exp\{-\nu[8\ln(d/a)\ln(2v_1/|\omega|a^*)]^{1/2}\}}{\omega[\ln(2v_1/|\omega|a^*)]^{1/2}}, \tag{47}$$

where C_1 is a constant. We see that as $\omega\to 0$, ${\rm Im}X_{\rm ret}(\omega)$ satisfies $\omega^{\delta-1}<{\rm Im}X_{\rm ret}(\omega)<\omega^{-1}$ for any positive δ. One can also easily check that $\int_0^{\omega_0}{\rm Im}X_{\rm ret}(\omega)d\omega$ is finite.

Now let us consider the behavior of the propagators for $1/d<k<1/a$. In this case $\theta_k\approx 0$ and the interedge interaction is not important. After taking the limit $d\to\infty$ we have

$$e^{-2\theta_k}=1,$$
$$\tilde{v}_k\approx\frac{\alpha c}{\epsilon\pi}\ln\frac{2}{ka} \tag{48}$$

at small k. We find surprisingly that $\langle\phi(0,t)\phi(0)\rangle$ has the same asymptotic behavior as that for a constant velocity: $\langle\phi(0,t)\phi(0)\rangle\to-\ln t^2+i\pi$. Thus repeating the calculations in the last section we find

$${\rm Im}X_{\rm ret}(\omega)\approx C_2\frac{|\omega|^{2\nu}}{\omega}, \tag{49}$$

where C_2 is a constant. The ratio C_1/C_2 can be determined by allowing the two curves (47) and (49) to connect smoothly around $k\sim 1/d$, or equivalently, around

$\omega \sim \omega_i = (e^2/\epsilon\pi d)\ln(d/a)$. Equation (47) is valid when $\omega \ll \omega_i$ and (49) when $\omega_i \ll \omega \ll e^2/\epsilon a$. ($e^2/\epsilon a$ is the high-energy cutoff of our effective theory.)

From the above discussion we find that the dc I_t-V_t curve for the $\nu=1$ IQH state in the presence of the Coulomb interaction has the following properties. For $e^2/\epsilon a \gg eV_t \gg \omega_i$, the I_t-V_t relation is linear and satisfies Ohm's law. When $eV_t < \omega_i$, the nonlinear behaviors start to appear and I_t/V_t increases as V_t decreases. In particular $I_t \to \infty$ as $V_t \to 0$. To get some rough idea about the shape of the I_t-V_t curve, we plot in Fig. 8 the curve as calculated from (47), (49), and (5). Due to the approximations we made in the calculations leading to (47) and (49), the curve is not completely reliable. But we expect the qualitative features, e.g., the divergences in I_t/V_t and I_t as $V_t \to 0$, are correct. Due to the singularity near $V_t=0$ in the I_t-V_t curve, we expect to see resonance structures similar to those in Fig. 7 when an ac component is present.

Let us make some numerical estimates. We may choose $d=2000$ Å, $a=200$ Å, and $\epsilon=10$. Then $e^2/\pi\epsilon d \approx 0.2$ meV. Thus the breakdown of Ohm's law will appear when $T < eV_t < 0.3$ meV (which requires $T \ll 3$ K). Such a condition is not difficult to achieve in experiments.

We also calculated the I_t-V_t curve for the $\nu=\frac{1}{3}$ FQH state with the Coulomb interaction. We find that the curve is very similar to that in Fig. 5, except I_t diverges faster when the Coulomb interaction is present. The qualitative behaviors represented in Figs. 5–7 should remain unchanged after the inclusion of the Coulomb interaction.

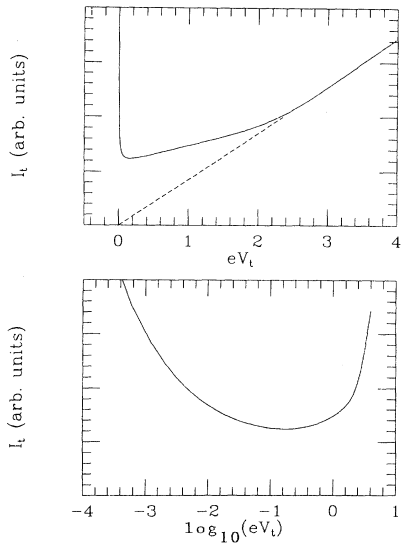

FIG. 8. The dc I_t-V_t tunneling curve for the $\nu=1$ IQH state in Fig. 4 with the Coulomb interaction at zero temperature. eV_t is measured in units of $e^2/\epsilon d$. We have chosen $d/a=10$.

III. RELATIONS TO ONE-DIMENSIONAL INTERACTING ELECTRON MODELS

In the preceding section we saw that when projected down to the first Landau level, the electron system presented in Fig. 4 can be mapped into a one-dimensional system. The column states in the Landau gauge in the quantum Hall system correspond to the momentum eigenstate in the 1D system. Notice that in the Landau gauge we have the translation symmetry in x direction. The column states are the eigenstates of the momentum in the x direction. The momentum k_x is related to the position of the column state through $k_x = y/l^2$, where y is the y coordinate of the center of the column state. If the electrons in Fig. 4 are confined by a smooth potential $V(y)$, then the Hamiltonian of the mapped 1D system is given by (for the free electrons)

$$H_0 = \sum_{k_x} V(k_x l^2) c^\dagger_{k_x} c_{k_x} . \tag{50}$$

The ground state of (50) is a Fermi liquid which corresponds to the IQH state with the first Landau level filled. In the presence of weak interactions the infrared fixed point of the system is described by the Luttinger liquid.[21]

When the electrons are interacting, the mapped 1D system also contains an interaction term. For a 2D electron interaction $V_{ee}(z_i - z_j) = \partial^2 \delta(z_i - z_j)$, the mapped interaction term in 1D is

$$H_1 = \sum_{k_1+k_2=k_3+k_4} V_{ee}(k_1,k_2,k_3,k_4) c^\dagger_{k_1} c^\dagger_{k_2} c_{k_3} c_{k_4} , \tag{51}$$

$$V_{ee}(k_1,k_2,k_3,k_4) \propto k_1k_4 + k_2k_3 - k_1k_3 - k_2k_4 .$$

Note that V_{ee} is regular for small k, hence it represents a local interaction in 1D. In fact one can easily show that (51) correspond to the following two-body interaction in 1D:

$$V_{ee}(x_i - x_j) = \partial^2 \delta(x_i - x_j) . \tag{52}$$

We know that in 2D when the electron interaction V_{ee} is much larger than the potential V, the electrons will form a new kind of state, e.g., the $\nu=\frac{1}{3}$ Laughlin state. This implies that, after the mapping, the 1D system described by H_0+H_1 also supports a new ground state when $H_1 \gg H_0$. It is interesting to see whether such a new state in 1D represents a new universality class or not. One way to address this problem is to study the electron propagator. According to the above mapping, the low-energy dynamics of the 1D system H_0+H_1 is described by the Kac-Moody algebra (18) and the Hamiltonian (30). The Hilbert spaces of the low-energy states are generated by[9] the density operators $\rho_{L,R}$, the charge e operators $e^{\pm i(\sqrt{q}/e)\phi_{L,R}}$ and the quasiparticle backscattering operators $e^{\pm i(1/e\sqrt{q})\phi}$. Here ϕ is equal to $\phi_R + \phi_L$ and $q = 1/\nu$ is an odd integer. In the presence of generic interactions the physical electron operators may mix with the quasiparticle backscattering operators. The electron operator may take the following general form:

$$c_{L,R}=\sum_{n=-\infty}^{\infty} A_n e^{\pm i(\sqrt{q}/e)[\phi_{L,R}+(n/q)\phi]} e^{\pm i(q+2n)k_F x} . \quad (53)$$

Actually (53) is the most general form of a local charge e operator. From (53) we see that the electron propagator has a form

$$G_e(x,t)\propto \sum_n (x\pm vt)^{q+2n}(x^2-v^2t^2)^{g_n^2} e^{\pm i(q+2n)k_F x} . \quad (54)$$

Equation (54) has structures identical to those of the electron propagator in the Luttinger liquid. Therefore the 1D state derived from the $\nu=1/q$ Laughlin state belongs to the same universality class as the Luttinger liquid derived from the $\nu=1$ IQH state.

We would like to point out that when $V=0$, the ground state and the low-lying excitations (i.e., the zero-energy sector) of the 1D Hamiltonian (which is H_1) are exactly soluble. Those zero-energy wave functions can be obtained by mapping the wave functions of the Laughlin state and the wave functions of the edge excitations[9,7,8] into one dimension. The mapping of the Laughlin wave function into 1D has also been discussed explicitly in Ref. 22. Notice that the 1D system described by H_1 contains only one length scale k_F^{-1} while the corresponding 2D FQH system contains two length scales d and l. What happens is that different 2D FQH systems with the same $k_F=d/l^2$ map into the same 1D system. This property is related to the fact that the 2D system, after being projected into the first Landau level, is invariant under separate scalings $x\to\eta x$ and $y\to\eta' y$ if the potential is given by $V(z_i-z_j)=\partial^2\delta(z_i-z_j)$. As a consequence of the above scalings we find that the FQH states for $d\gg l$ and for $d\ll l$ are continuously connected to each other and have the identical excitation spectrum once $k_F=d/l^2$ is fixed. When $d\ll l$ the magnetic field is not important and the system reduces to the 1D model described by H_0+H_1. Many results obtained in this paper for the FQH effects also apply to such a 1D system. Since the CDW order parameter has a slow algebraic decay, $x^{-2/q}$, we may call the 1D state derived from the $\nu=1/q$ FQH states a CDW state.

Certainly in 1D one can only directly measure the I-V_{SD} curve (see Fig. 5). For $V_{SD}\gg V_{SD0}$ and at $T=0$, the conductance is given by $I/V_{SD}=ge^2/h-\gamma V_{SD}^{2g-2}$ where γ is a constant. In the presence of an ac component in current I, the dc part of $V_{SD}(t)$ can easily be calculated from (27) and Fig. 7. The results are presented in Fig. 9. The resonances appear when the current is equal to a multiple of $e\Omega/2\pi$. Those resonances can easily be understood from a CDW picture. Actually the steps similar to those in Fig. 7 have been observed in three-dimensional CDW states.[23] Notice that the resonances happen at such currents that an integer number of electrons are transported through the system in each period $2\pi/\Omega$. We know when a CDW state (or a state with strong CDW fluctuations) passes through an impurity, the density oscillation in space will cause an oscillation in time. If there is one electron in each period of the CDW state, the frequency of the oscillation will be $\Omega_0=2\pi I/e$. This oscillation, when resonant with the external oscillation, causes the first step in Fig. 9. The other steps are caused by the resonances with higher harmonics in the external oscillations. It is very satisfying to see that the result of the quasiparticle tunneling in the

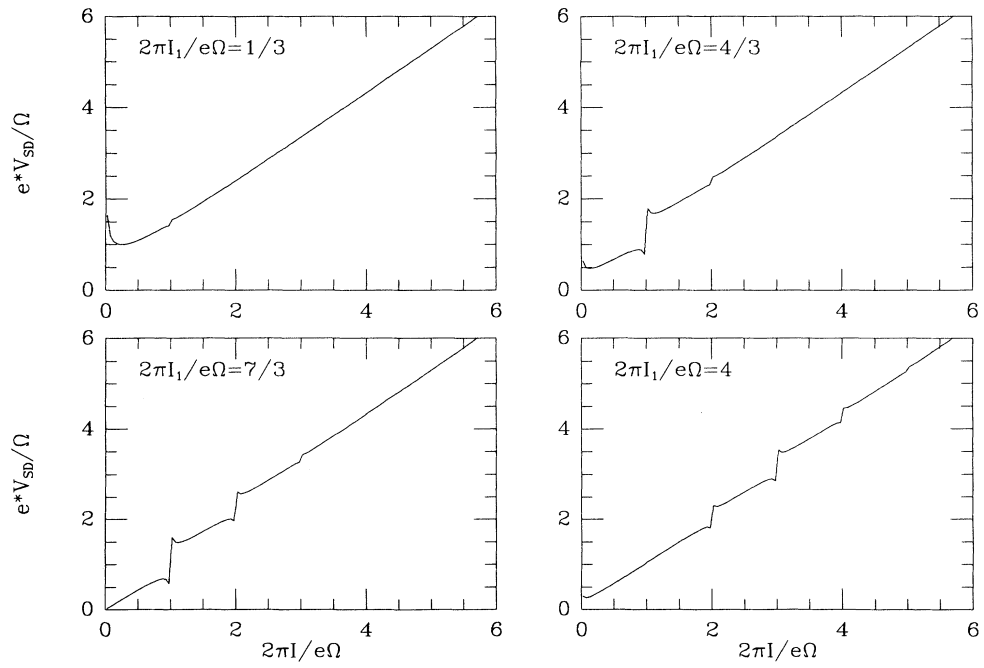

FIG. 9. The dc part of the I-V_{SD} curve for the CDW state or the $\nu=\frac{1}{3}$ Laughlin state in Fig. 4. I contains an ac component: $I(t)=I+I_1\sin(\Omega t)$. The temperature T is chosen to be zero.

FQH states can be explained by the above simple CDW picture. This also confirms that the transport properties of the FQH states are governed by the quasiparticle tunneling.

We would like to remark that in 3D CDW samples, one also observed steps at rational values of $2\pi I/e\Omega$. Those new steps can be obtained in our model by including higher-order terms of Γ in the tunneling formula (1).

We would like to mention that the limit $d/l \to \infty$ (with $k_F = d/l^2$ fixed) is very useful. In this case the FQH state is a well-defined bulk state and yet equivalent to the 1D system described by H_1. Many properties of the 1D system described by H_1 can be obtained in this limit from the known properties of the FQH effects. For example, it is clear that the electron propagator in the FQH state only contains singularities at $\pm 3k_F$. This implies that after mapping to 1D the electron operators take the simple form

$$c_{L,R} = e^{\pm i(\sqrt{q}/e)\phi_{L,R}} e^{\pm iqk_F x} . \tag{55}$$

The k_F singularity disappears.

IV. DISCUSSION

Before ending the paper we would like to discuss the limitations and the approximations in our approaches. All the results obtained in this paper are based on the low-energy effective Hamiltonian (22) or (30). The complete Hamiltonian may contain many other terms, e.g., the anharmonic term $\sum \rho_{k_1}\rho_{k_2}\rho_{-k_1-k_2}$. Those terms are irrelevant at low energies and can be ignored if we are only interested in the low-energy properties of the system. Thus our results are correct only when k and ω are less than certain cutoff values. In the following we will discuss the values of the momentum and the frequency cutoff in the effective theory.

If electrons experience only a short-range interaction with a range less than the electron separation $n^{-1/2}$, then the momentum cutoff a^{-1} is expected to be of order $n^{1/2} = \sqrt{\nu/2\pi}\, l^{-1}$. For a 10-T magnetic field a is of order 100 Å. In the presence of the Coulomb interaction the situation is more complicated. When the cyclotron frequency ω_c is much larger than the characteristic Coulomb energy $\epsilon_{cl} = \sqrt{\nu/2\pi}(e^2/\epsilon l)$, experimental value of the gap is of order 1 K for the $\nu = \frac{1}{3}$ FQH state. We may take Δ as the energy cutoff of our effective theory. The momentum cutoff may be determined from $\Delta = k(e^2/\epsilon\pi)\ln(2/ka)|_{k=1/a}$, which gives $a \sim e^2/\Delta\pi \sim 3000$ Å. For the $\nu = 1$ IQH state, we would choose $\Delta \sim \omega_c$. In this case $e^2/\Delta\pi$ is less than the interelectron distance. So the cutoff scale is given by the latter: $a \sim 2.5l \sim 200$ Å at $B = 10$ T. We would like to point out that the above estimates (and other numerical estimates in the paper) are very crude. They may be off by a factor of 3 or more.

The results obtained in this paper also apply to the hierarchical FQH states, because the Green function of the electron or the quasiparticle on edge also has a form[11]

$$G(x=0, t) \propto t^{g} .$$

The value of the exponent g depends on the detail structure of the hierarchical state.

In this paper we discussed the transport properties of the edge states in the IQH and FQH effects, with or without Coulomb interactions. We find that the transport properties demonstrate various nonlinear or even singular behaviors. Those behaviors can be used to directly measure the fractional charges of the quasiparticles. We also find that the interedge interactions have profound effects on the edge transport properties of the QH states, sometimes quantitatively and sometimes even qualitatively. In many cases the interedge interactions complicate the matters. One way to avoid the interedge interactions is to do experiments on samples with a geometry as illustrated in Fig. 10. Many predictions that we obtained here are within the reach of the present experimental technology. It would be very interesting to test those predictions in experiments.

We also discussed the scattering of a moving 1D CDW state (i.e., a state with an algebraically decaying CDW order parameter) by a single weak impurity. We find that the differential conductance of the system is given by

$$\frac{dI}{dV_{SD}} = g\frac{e^2}{h} + \gamma V_{SD}^{2g-2} \tag{56}$$

when V_{SD} is much larger than the pinning threshold but much less than the cutoff v/a. Here ge^2/h is the conductance of the CDW state in the absence of impurities and γ is a constant. We find that the conductance of the clean system determines the exponent in (56). The pinning threshold for a weak impurity can be estimated from (28). We see that the pinning threshold has a nontrivial power-law dependence on the impurity strength.

We have been emphasizing the similarity between 1D CDW systems and 2D FQH systems. Certainly there are differences between the two systems. For example, the narrow-band noise in the dc transport still exists even

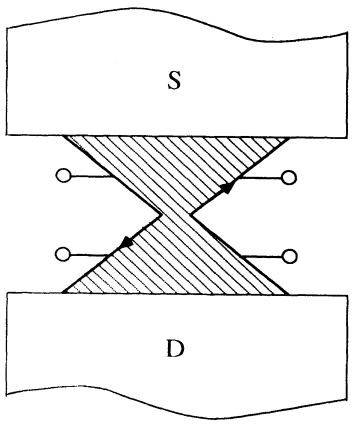

FIG. 10. A sample geometry which reduces the effects of interedge interactions.

when the 2D FQH system is not 1D like, say with a geometry given in Fig. 10. In this case it is hard to use the spatial charge modulation to explain the narrow-band noise. Also in this case the exponents g in (8) and (56) are quantized and take simple rational values.

ACKNOWLEDGMENTS

I would like to thank T. M. Rice for a helpful discussion. This work was supported by the Department of Energy Grant No. DE-FG02-90ER40542.

*Present address: Department of Physics, MIT, Cambridge, MA 02139.

[1]B. I. Halperin, Phys. Rev. B **25**, 2185 (1982).
[2]X. G. Wen, Phys. Rev. B **43**, 11 025 (1991).
[3]A. H. MacDonald, Phys. Rev. Lett. **64**, 220 (1990).
[4]P. Streda, J. Kucera, and A. H. MacDonald, Phys. Rev. Lett. **59**, 1973 (1987); M. Büttiker, Phys. Rev. B **38**, 9375 (1988).
[5]J. K. Jain and S. A. Kivelson, Phys. Rev. B **37**, 4276 (1988); Phys. Rev. Lett. **60**, 1542 (1988).
[6]X. G. Wen, Phys. Rev. Lett. **64**, 2206 (1990).
[7]M. Stone (unpublished); Int. J. Mod. Phys. B **5**, 509 (1991).
[8]D. H. Lee and X. G. Wen, Phys. Rev. Lett. **66**, 1765 (1991).
[9]X. G. Wen, Phys. Rev. B **41**, 12 838 (1990).
[10]F.D.M. Haldane, Bull. Am. Phys. Soc. **35**, 254 (1990).
[11]X. G. Wen, Mod. Phys. Lett. B **5**, 39 (1991); B. Blok and X. G. Wen, Phys. Rev. B **42**, 8133 (1990); **42**, 8145 (1990).
[12]X. G. Wen, Phys. Rev. Lett. **66**, 802 (1991).
[13]A. Balatsky and M. Stone, Phys. Rev. B **43**, 8038 (1991).
[14]K. B. Efetov and A. I. Larkin, Zh. Eksp. Teor. Fiz. **72**, 2350 (1977) [Sov. Phys.—JETP **45**, 1236 (1977)]; H. Fukuyama and P. A. Lee, Phys. Rev. B **17**, 535 (1978); A. I. Larkin and P. A. Lee, *ibid.* **17**, 1596 (1978); P. A. Lee and T. M. Rice, *ibid.* **19**, 3970 (1979), and references cited therein.
[15]S. E. Barnes and A. Zawadowski, Phys. Rev. Lett. **51**, 1003 (1983); I. Tutto and A. Zawadowski, Phys. Rev. B **32**, 2449 (1985).
[16]J.H.F. Scott-Thomas *et al.*, Phys. Rev. Lett. **62**, 582 (1989); U. Meirav, M. A. Kastner, and S. J. Wind, *ibid.* **65**, 771 (1990).
[17]J. R. Schrieffer, D. J. Scalapino, and J. W. Wilkins, Phys. Rev. Lett. **10**, 336 (1963).
[18]R. Shankar, J. Mod. Phys. B **4**, 2371 (1990).
[19]P. A. Lee, Phys. Rev. Lett. **65**, 2206 (1990).
[20]W. Apel, J. Phys. C **15**, 1973 (1982); T. Giamarchi and H. J. Shultz, Phys. Rev. B **37**, 325 (1988).
[21]J. M. Luttinger, J. Math. Phys. **15**, 609 (1963); D. C. Mattis and E. H. Lieb, *ibid.* **6**, 304 (1965); E. H. Lieb and D. C. Mattis, *Mathematical Physics in One Dimension* (Academic, New York, 1966), Chap. 4; A. Luther and I. J. Peschel, Phys. Rev. B **9**, 2911 (1974); Phys. Rev. Lett. **32**, 992 (1974); A. Luther and V. J. Emery, *ibid.* **33**, 589 (1974); A. Luther, Phys. Rev. B **19**, 320 (1979); F.D.M. Haldane, J. Phys. C **14**, 2585 (1981); G. D. Mahan, *Many-Particle Physics* (Plenum, New York, 1981), p. 311.
[22]E. H. Rezayi and F.D.M. Haldane (unpublished).
[23]P. Monceau, J. Richard, and M. Renard, Phys. Rev. Lett. **45**, 43 (1980); S. Brown, G. Mozurkewich, and G. Grüner, *ibid.* **52**, 2277 (1984); Z. Z. Wang *et al.*, Solid State Commun. **46**, 325 (1983).